EFDA–JET–PR(07)63

Yu.F. Baranov, I. Jenkins, B. Alper, C.D. Challis, S. Conroy, V. Kiptily,
J. Ongena, S. Popovichev, P. Smeulders, E. Surrey, K-D. Zastrow
and JET EFDA contributors

Anomalous and Classical Neutral Beam Fast Ion Diffusion on JET

Anomalous and Classical Neutral Beam Fast Ion Diffusion on JET

Yu.F.Baranov[1], I.Jenkins[1], B.Alper[1], C.D.Challis[1], S.Conroy[2], V.Kiptily[1], J. Ongena[3], S.Popovichev[1], P.Smeulders[4], E.Surrey[1], K-D.Zastrow[1] and JET EFDA contributors*

JET-EFDA, Culham Science Centre, OX14 3DB, Abingdon, UK

[1]EURATOM-UKAEA Fusion Association, Culham Science Centre, OX14 3DB, Abingdon, OXON, UK
[2] Deptartment of Neutron Research, Uppsala University, Uppsala, Sweden, EURATOM-VR
[3]Association "EURATOM-Belgian State", Brussels, Belgium, TEC Partner
[4]Associazione EURATOM/ENEA sulla Fusione, Centro Ricerche Frascati c.p. 65, 00044 Frascati, Italy
** See annex of M.L. Watkins et al, "Overview of JET Results ",*
(Proc. 21 st IAEA Fusion Energy Conference, Chengdu, China (2006)).

Preprint of Paper to be submitted for publication in
Nuclear Fusion

ABSTRACT

Trace Tritium Experiments (TTE) on JET were analysed using Monte Carlo modelling of the neutron emission resulting from the Neutral Beam Injection (NBI) of short (~300ms) Tritium (T) beam blips into reversed shear, hybrid ELMy H-mode and L-mode deuterium plasmas for a wide range of plasma parameters. The calculated neutron fluxes from Deuterium-Tritium (DT) reactions could only be made consistent with all plasmas by applying an artificial reduction of the T beam power in the modelling of between 20 and 40%. A similar discrepancy has previously been observed in both JET [1] and TFTR [2], although no mechanism has yet been found that could explain such a difference in the measured T beam power. Applying this correction in the T beam power, good agreement between calculated and measured DT neutron emission profiles was obtained in low to moderate line averaged density ($\bar{n}_e < 4\times10^{19}\,m^{-3}$) ELMy H-Mode plasmas assuming that the fast beam ions experience no, or relatively small, anomalous diffusion ($D_{an}<<0.5m^2/s$). However, the modelled neutron profiles do not agree with measurements in higher density plasmas using the same assumption and the disagreement between the measured and calculated shape of the neutron profile increases with plasma density. In this paper it is demonstrated that large anomalous losses of fast ions have to be assumed in the simulations to improve agreement between experimental and simulated neutron profiles, characterized by the goodness of fit. Various types of fast ion losses are modelled to explain aspects of the data, though further investigation will be required in order to gain a more detailed understanding of the nature of those anomalous losses.

1. INTRODUCTION

The understanding of fast ion physics in tokamak plasmas is important for modelling and interpretation of neutral beam injection experiments. It is required for the derivation of transport coefficients and for the simulation of heating and current drive in beam heated plasmas and is thus important for extrapolation to ITER.

Various models exist to describe fast ion behaviour, such as those implemented in the TRANSP [3] Monte Carlo code. However, such simulations do not always reproduce experimental effects, as is the case on ASDEX Upgrade [4] and on DIII-D [5,6], where it has been necessary to introduce an anomalous radial diffusion of the fast ions in the model for the beam-driven current in order to match the measured data.

In addition to determining thermal tritium transport coefficients, the JET TTE campaign [7] allowed an examination of fast ion physics using two dedicated T NB injectors, one for on-axis and one for off-axis injection [8]. This removes uncertainties about the amount of T delivered by the injector, which may occur if T doping is used, as was the case in a previous campaign. Also, in the experiments discussed in this paper, no T gas puff was used. This leads to greater confidence in determining the concentration of thermal T present in the plasma and also lowers any recycling of T from previous pulses, resulting in low DT neutron emission in the D heating phase before the T blip. This also has not been the case in previous T campaigns on JET.

This paper describes experiments in which short (~300ms) T beam blips were injected into various D plasmas with various configurations, such as reversed shear plasmas with a current-hole [9,10], the 'hybrid scenario' [11] (which is characterised by a monotonic q profile), as well as standard ELMy H-mode and L-mode plasmas. The JET 2-D neutron camera [12,13,14] (see Fig.1) was used to provide time and space resolved neutron emission profiles from DT fusion reactions resulting from the injected fast T atoms. The camera measures line-integrated neutron emission fluxes along horizontal and vertical lines of sight. The systematic error for the 14MeV neutron measurement is ~10% with a statistical error of ~3-5% [15]. These measurements are compared with simulated neutron fluxes along those same sightlines, obtained by the Monte Carlo code in TRANSP, which contains a rather detailed description of the physical processes involved in the fast particle dynamics, including gyrokinetic orbit effects.

In this paper comparisons are made between measured and modelled line integrated neutron emission profiles in JET. Simulations are done with and without anomalous diffusion for the fast T particles to check the validity of the classical fast ion physics model, as implemented in TRANSP, for a large variation in plasma parameters.

2. NEUTRAL BEAM PARTICLES IN REVERSED SHEAR AND HYBRID SCENARIO DISCHARGES.

Strong neoclassical effects can lead to a peculiar behaviour of the fast ions in reversed shear plasmas with a current hole. This section begins with a discussion of the results obtained for such plasmas as it illustrates the sensitivity of the neutron profile measurements to the plasma configuration and the capability of TRANSP to model fast ion behaviour. The tritium beam was switched on during a short period of time $6s<t<6.3s$, in the presence of 12MW of deuterium Neutral Beam Injection (NBI) and 4MW of Ion Cyclotron Resonance Heating (ICRH) at a plasma current $I_P = 2.35MA$ and magnetic field $B_t = 3.2T$. LHCD was applied early in the current ramp-up phase ($1.5s<t<4s$) to create a reversed shear configuration with a current hole [9]. At the time of the tritium beam blip the density in the plasma centre reached $n_e(0) = 4.5\times10^{19}\ m^{-3}$, (a Greenwald fraction $\bar{n}_e/n_{gr} = 0.32$, where the Greenwald density limit $n_{gr} = I_p(MA)/(\pi*a^2)$ [16]) and the line averaged density was $\bar{n}_e = 2.6\times10^{19}\ m^{-3}$. Strong electron and ion ITBs (i.e. those with normalised electron and ion gyroradii, $\rho^*_{e,i} > 0.2$ [17]) have been formed at the time of T beam blip.

To demonstrate the sensitivity of the modelling to variations in the diffusion of the fast ions, a comparison of measured and calculated plasma stored energy W_{dia} (determined using a diamagnetic loop) and total neutron yield is shown in Figs.2 and 3, for two cases: (i) Purely (neo)classical fast ion behaviour (no anomalous diffusion) and (ii) fast ions subjected to an anomalous diffusion $D_{an} = 0.5m^2/s$ (constant in space and time). The value of $D_{an} = 0.5m^2/s$ is in the typical range for the core of a plasma not having a transport barrier. In the absence of anomalous diffusion, we find agreement with the experimental data within the uncertainties on the measurements. For the case where $D_{an} = 0.5m^2/s$ is assumed, the main difference between the two simulations is that the fast ion

contribution is about 20% smaller than in the previous case, resulting in a larger discrepancy between simulated and experimental values for to W_{dia}. A small difference in the thermal energy is caused by a difference in the flux surface equilibrium reconstruction, as the location of the magnetic axis is shifted by 3-4cm to the low field side in the case of zero D_{an} due to the higher fast ion contribution in the total plasma pressure.

The interpretation of the phase preceding the T beam pulse is essential for an accurate and consistent modelling of the T beam blip phase. The plasma composition was deduced from charge-exchange measurements of Carbon, Iron, Nickel and Copper concentrations. Fig.3a shows an evolution of the total and 14MeV neutron flux in the deuterium NBI phase where 14MeV (DT) neutrons contribute for about 10% to the total flux. This neutron emission occurs due to recycling of the residual tritium from the wall. Reasonable agreement between the measured and calculated DT neutron flux in this phase (see Fig.3a) was obtained assuming that the flux of T neutrals is of the order of $10^{-3} - 10^{-4}$ of the flux of D neutrals from the wall. As the magnitude of the DT emission is small compared to that of the DD neutron emission in the phase before the T beam blip, it is clear that the DT neutron flux is completely dominated by T beam onto D fusion reactions during the T blip. Fig.3b shows the total neutron flux and that from DT reactions during and just after the T blip. Here TRANSP overestimates the 14MeV neutron flux, a very similar result having been observed in previous experiments using T beam injection on JET [1] and TFTR [2]. However, the time evolution of the neutron yield can be satisfactorily reproduced by artificially reducing the T beam power by 0.77 for the case of zero anomalous diffusion, as illustrated by a dashed line in Fig.3b. The power reduction is simply equivalent to a reduction of the number of fast neutrals injected into the plasma. A detailed examination of off-line T NB pulses (necessarily limited in number due to constraints in T usage) with corresponding D pulses compared the total energy deposited onto the beamline calorimeter with each beam species. This found a statistical error of approximately 12% for the T power from both T beam injectors relative to the D power. The reduction in T power of 23% to reach agreement in this case is twice this error in the T power. The required reduction in power for this pulse (and subsequent pulses discussed later in this paper) prompted an investigation in the pressure response of the NB beam line during the T pulses in order to observe any possible reduction in neutralisation efficiency which could account for such a reduction in power. No evidence of such a pressure reduction, or any other possible mechanism which may explain the required power reduction in the modelling, was found.

The behaviour of fast beam particles is sensitive to the q-profile [18]. Proper modelling of the fast particles therefore requires an accurate description of the magnetic topology. To validate the equilibrium used, a comparison was made of the calculated and measured (by the MSE diagnostic [19]) pitch angle $\alpha = B_p/B_t$, where B_p and B_t are poloidal and toroidal components of the magnetic field. Results of the comparison are presented in Fig.4. We find a good agreement both for the magnitude of the total neutron flux and the shape of the neutron profiles. The flattening of the parameter α in the region $2.8m<R<3.25m$ indicates a zone of zero or very small plasma current

density, corresponding to a reversed shear configuration with a current hole. The q-profile corresponding to such configuration is also shown in Fig.4 for two time slices as simulated by TRANSP. It should be noted that the q-profile as well as the pitch angle α were derived self consistently by solving the plasma equilibrium taking into account the evolution of the plasma pressure and poloidal field diffusion. The initial conditions were deduced from EFIT at the start of LHCD preheat, when the total plasma current is relatively small. However, the dependence of the q-profile on the initial conditions in the current flat top phase is weak as the q-profile strongly changes due to the application of LHCD in the current ramp-up phase.

The evolution of the measured and calculated neutron emission for JET Pulse No: 61341 along the 19 lines of sight of the neutron camera (see Fig.1) is shown in Fig.5 during and after the T beam blip for the pulse discussed so far in this section. The modelled tritium beam power was reduced by 23% to achieve agreement between the evolution of the calculated and measured 14MeV neutron fluxes, as discussed above. Under these conditions, reasonable agreement between the calculated and measured profiles can also be obtained (see Fig.5) for the case of zero anomalous diffusion. This agreement is less good when a relatively small fast ion anomalous diffusion $D_{fast} = 0.5m^2/s$ is introduced in the modelling.

A more accurate comparison of the simulated and measured profiles during the time interval Δt of the ΔT beam blip can be performed by calculating $\chi^2 = (\ t)^{-1} \int_{t=t_0}^{t=t_0+\Delta t} \sum_{i=1}^{19} dt\ (f_i(t) - f_i^{\,0}(t))^2/\sigma_i^{\,2}(t)$, where $f_i(t)$ and $f_i^{\,0}(t)$ are, respectively, modelled and measured neutron fluxes along 19 different lines of sight (each corresponding to a separate channel in the neutron camera) and $\sigma_i^{\,2}(t)$ are corresponding standard deviations deduced from the statistical error bars of the measurements. Due to the uncertainty in the magnitude of the injected T beam power $P_{T,}$ the value for P_T used in the modelling was varied in order to minimise χ^2. This process was repeated for cases with different anomalous diffusion coefficients D_{an} in order to find whether cases with or without anomalous diffusion in the model gave a lower χ^2 (and hence a better fit to the data). The minimum value for $\chi^2 = 6.73$ was found for the case of zero D_{an}, and it increased significantly to 15.1 when assuming $D_{an} = 0.5m^2/s$. Just after the start of the T beam blip, the maximum emissivity in the measured line integrated neutron emission profile was observed near channel #16, as shown in Fig.5. After the T beam has been switched off, the peak moves to channel #15. This interesting feature, its theoretical prediction [12] having been confirmed in experiment [11], is linked to the presence of the current hole. The successful reproduction of this subtle neo-classical effect proves the validity of the modelling. It should be stressed that this feature is reproduced quite satisfactorily in the modelling assuming that $D_{an} = 0$, but that this good agreement disappears when $D_{an} = 0.5m^2/s$ is assumed. Thus, this observation indicates that any fast anomalous diffusion must be relatively small (i.e. $D_{an} << 0.5m^2/s$).

It is instructive to compare the effect of fast ion neoclassical and anomalous diffusion on the beam driven currents I_{nb}. Figure 6 shows such comparison for Pulse No: 61341. About 10% reduction in I_{nb} is caused by the introduction of a relatively small anomalous diffusion ($D_{an} = 0.5m^2/s$). The beam

driven current profile is affected much stronger in the plasma core, where it decreases by 50%.
A better understanding of the relation between the fast beam particles and the neutron profiles can be reached by analysing the fast ion distribution function and the plasma fusion reactivity. Figure 7a shows the dependence of $\langle\sigma^*v\rangle = \int F_D(D)\sigma(|\vec{v}_b - \vec{v}|)|\vec{v}_b - \vec{v}|dv$ for the DT reaction with beam tritons at velocity v_b in a deuterium plasma characterized by a Maxwellian distribution function $F_D(v)$ calculated with cross-sections from [20]. The modelled fast ion distribution function $F_T(E)$ from TRANSP versus ion energy E is shown in Fig.7b for 100keV tritons injected on-axis in Pulse No: 61341 assuming neoclassical diffusion for the ions ($D_{an} = 0$). The distribution function is averaged over the poloidal angle ($0<\theta<2p$), pitch angle ($-1<V_{//}/V<1$) and part of the minor radius ($0.1<r/a<0.3$). Different time slices are shown to demonstrate the time evolution of the distribution function. A comparison of the curves corresponding to the two latest slices (t = 6.225s and 6.3s) shows that the T distribution function has not reached the steady state by the end of the T beam blip (t = 6.3s) although the difference between t = 6.2 and t = 6.3s is rather small. Variations in the plasma density and electron temperature will affect the distribution function and the time scale of its evolution. The differential reactivity $dR/dE = F_T(E)n_d\langle\sigma^*v\rangle$ and total reactivity $R = \int (dr/dE)dE$ are shown for the nearly steady state T distribution function in Fig.7c and d. Both R and its derivative dR/dE show that the neutron emission is dominantly produced by the high energy part of the beam distribution function. This confirms that the evolution of the spatial distribution of fast tritons can be detected by the observation of 14MeV neutrons originating from fast tritons in the high velocity part of the energy distribution function where the DT reaction probability is high.

The simulations provided also more detailed information about the fast tritium distribution function, important for the interpretation of the shape of the measured neutron emission profiles. Figure 8a shows the evolution of the calculated fast tritium ion density during the T beam blip. By definition in TRANSP, fast ions are considered such if their energy is greater than 1.5 times that of the thermal ions. It should be noted that the source function of the fast ions is more peaked than the subsequent fast ion density profiles. The fast triton density profile closely approaches, but does not reach the steady state during the T beam blip. Figure 8b and c show the fast triton distribution function by the end of the blip. It is strongly anisotropic, as much more particles move in the positive co-beam direction $0<V_{//}/V<1$ (in the direction of the plasma current and magnetic field) than in the opposite direction $-1<V_{//}/V<0$ (see Fig. 8b). The amount of the tritons above 70keV is significantly larger in the toroidal segment $0.1<r/a<0.3$, $-0.5\leq\theta\leq0.5$ on the LFS than in the segment $0.1<r/a<0.3$, $\pi-0.5\leq\theta\pi\leq+0.5$ on the HFS (see Fig.8c). This imbalance is due to trapping of fast ions in the vicinity of the "stagnation" point [10], occurring in the region where the poloidal field is very small, associated with the "current hole" configuration. In this point the poloidal velocity of the fast ion guiding centre tends to zero due to a compensation of the downward toroidal drift by the upward movement along the magnetic field line. These "trapped" tritons are responsible for the asymmetry in the profiles of the neutron flux measured by the vertical camera (Fig.1). The signal of channel 14 signal is considerably smaller than the signal in channel 16 during the whole duration of the T beam

pulse 6s<t<6.3s. The asymmetry disappears about100ms after the switch-off of the T beam. This time is on the order of the pitch angle scattering time of the fast ions.

Qualitatively very similar results have been found in the case of a 'hybrid scenario' [11] discharge, which is characterised by a monotonic q profile with q(0) >1. A tritium beam blip was injected in this plasma at B_t = 2.4T and I_p = 2MA during the main heating phase, consisting of 15MW deuterium NBI and 1MW ICRH. At the time of the T beam pulse the central plasma density was $n_e(0) = 4.3\times10^{19}$ m^{-3} (Greenwald fraction $\bar{n}_e/n_{gr}$ = 0.4) and line averaged density $\bar{n}_e(0) = 2.9\times10^{19}$ m^{-3}. Neoclassical Tearing Modes (NTM) (m/n=1/1, 3/2, 4/3) and ELM activity was present during the T beam blip phase, but no sawteeth, fishbones or TAE modes. The largest T_e perturbations caused by the NTMs were localised in the core region (0.1<r/a<0.5).

The TRANSP simulation again reproduces the total neutron yield evolution quite well in the phase preceding the T beam blip (within the 10% measurement uncertainty). The total calculated neutron flux, including the 14MeV neutron emission during the T beam blip exceeds the measured emission by 30%. As before, an artificial reduction of the tritium NBI power by 30% in the simulation eliminates this discrepancy. Calculated and measured profiles of 14MeV neutron emission are shown in Fig. 9 with and without fast ion anomalous diffusion in the simulation. An anomalous ion diffusion coefficient $D_{an} = 0.5m^2/s$ was assumed in the region 0.1<r/a<0.5, mimicking the effect of the observed MHD, which was localised in this region. As in the previous case the introduction of anomalous diffusion degrades the agreement between the calculated and measured profiles, which is reflected in the increase of min(χ^2) from 4.13 for D_{an} = 0 to 6.74 for $D_{an} = 0.5m^2/s$. The lowest value for minimum of χ^2 = 3.96 is achieved for relatively small D_{an} (= $0.1m^2/s$).

3. MODELLING OF 14MEV DT NEUTRON PROFILES FOR LOW TO INTERMEDIATE DENSITY PLASMAS (N/NGW <0.6) WITH A MONOTONIC Q PROFILE.

The disagreement between the experimental 14MeV DT neutron rate and the one simulated by TRANSP was further investigated in a sequence of plasmas with monotonic q profiles, reducing the complexity of the simulation.

In JET Pulse No: 61237 and 61238 (B_t = 3T, I_p = 1MA, $q_{95} \approx 8.5$) only a T beam blip was applied without any other additional heating. These discharges therefore remained in L mode throughout. The lack of beam power, and consequent low recycling from the wall, led to a low plasma density, ($n_e(0) = 1.6\times10^{19}$ m^{-3} $\bar{n}_e/n_{gr}$ = 0.35) at the time of the T blip. The plasma composition of the discharge was determined in the same way as the previous discharge. Figure10 shows that the 14MeV neutron rate is satisfactorily modelled if the T power is reduced by 40% for 61237 (off-axis) and 20% (on-axis) for 61238. These reduction factors are similar to the ones used in the previous section, though much larger than the uncertainty in the T beam power.

Additional tests of the model have been done analysing on- and off-axis T blips in standard H-mode Pulses No's: 61235 and 61236 (at B_t = 3T, I_p = 1MA, $q_{95} \approx 8.5$), which have a relatively low density of $n_e(0) = 3.0\times10^{19}$ m^{-3}, ($\bar{n}_e/ n_{gr}$ = 0.6) at the time of the T blip. An additional 12MW of D

beam heating power was used. Figure 11a shows that the total neutron rate is satisfactorily modelled by TRANSP for Pulse No's: 61235 and 61236 if the tritium power is reduced by 30% and 20%, respectively. The neutron profiles for these shots, integrated from 8.7s to 8.8s (see Fig.11b), show general agreement between measurement and simulation. Introducing an anomalous fast ion diffusion coefficient $D_{an} = 0.5m^2/s$ degrades agreement for both neutron rate and profile shape. A χ^2 analysis of the data was performed over a 100ms integration period and the profiles shown in Fig. 11 are averaged over this period. The error bars shown in the figure, however, correspond to a single profile (integrated over 10ms) in order to give an idea of the statistical error in a single measurement. We find that min(χ^2) increases in both discharges, when anomalous diffusion is assumed : for Pulse No: 61236 from min(χ^2) = 2.89 ($D_{an} = 0$) to 3.25 ($D_{an} = 0.5m^2/s$) and similarly for Pulse No:61235 from min(χ^2) = 6.31 ($D_{an} = 0$) to 22.34 ($D_{an} = 0.5m^2/s$).

Results of modelling of the neo-classical orbit effects are illustrated in Fig. 12, where the tomographically inverted 2D neutron profile from Pulse No: 61237 at time 6.25s is compared with the 2D fast ion distribution as calculated by TRANSP and plotted on an up-down symmetric equilibrium.

The asymmetrical peaking in the neutron emissivity at the high field side is explained by the accumulation of fast trapped ions in the vicinity of the 'banana' orbit tips. As the perpendicular component of the fast ion velocity reduces at the turning point of the trapped orbit, this results in a local increase of the fast ion density at this point and hence the neutron emissivity.

Summarizing the last two sections, we find that TRANSP provides a good simulation of the total measured flux in the D beam phase before the beam blip. TRANSP accurately describes the shape and the time evolution of 14MeV neutron emission profiles in discharges with different magnetic configurations and low to intermediate densities. The neutron emission is mainly from beam-beam and beam-plasma interactions. We have shown that neoclassical effects which strongly affect fast ion behaviour (in reversed shear discharges in particular) are correctly modelled in TRANSP. There is a discrepancy in the total calculated and measured neutron flux during the T blip. To get agreement we needed to reduce the T beam power in the simulation by 20-40% in the cases shown above. These reduction factors are much larger than the error bar in the T beam power, as was also observed earlier in JET and TFTR. Up to now no mechanism has been proposed which offers an explanation for this reduction.

It should be noted that no artificial reduction was needed in the simulations for the T beam power [1,2] in the interpretation of the results of previous campaigns (PTE and DTE) [21,22] as the neutron yield was dominated by the interaction of the thermal ions and beam-target and beam-beam neutrons made up a considerably smaller part of the total neutron yield. The uncertainty in Z_{eff} as well as in relative T and D concentrations of the plasma allows reaching agreement between experiment and modelling within the error bars.

In the next section we present the results of our investigations on neutron emission and fast ion behaviour in discharges with higher density.

4. MODELLING OF HIGH DENSITY H-MODE DISCHARGES.

The reversed shear and hybrid scenario plasmas discussed above are characterised by relatively low density ($n_e(0)<5\times10^{19}m^{-3}$, $\bar{n}_e/n_{gr} \leq 0.6$). Higher density ($n_e(0)>5\times10^{19}m^{-3}$, $0.6<\bar{n}_e/n_{gr}<1.1$) can be reached in ELMy H-mode plasmas, and this regime typically exhibits MHD behaviour not seen in either of the other regimes. The list of pulses analysed and their key parameters are given in Table 1 (we included the hybrid scenario Pulse No: 61158 discussed in the first section for comparison). The q-profile is monotonic in all pulses. Sawteeth and n = 1,m = 1 precursor oscillations were observed in all but one pulse. They were located in the region $0.3<r/a<0.4$. A smaller amplitude n = 2 mode was also observed. NTMs with m/n = 1/1, 3/2, 4/3 were present in Pulse No: 61158.

Figure 13a shows the measured 14MeV neutron emission profiles for the different pulses listed in Table 1. With increasing density, the profile measured by the horizontal neutron camera (channels 1-10) broadens and eventually becomes hollow as the density rises; the profile from the vertical camera (channels 11-19) shows less broadening and becomes asymmetric with increasing density. The increase in neutron emission with increasing density along the lines of sight at the Low Field Side (LFS) is much stronger than for the channels on the High Field Side (HFS). Note that the profiles shown in Fig.13 were obtained by averaging the data over 50ms at the end of the T beam blip. The effect of the sawtooth crash on the profiles can be neglected as the observation interval started at least three fast ion slowing down times after the last crash in all but one pulse (Pulse No: 61432), but even there the delay is still about two slowing down times.

A comparison of the normalised measured and calculated neutron emission profiles is shown in Fig.13 b-f. The calculated profiles correspond to the case of zero anomalous diffusion of the fast ions. The shape of the profiles is well reproduced in the case of plasma with the lowest density (Pulse No: 61158). As the density increases, the difference in shape between measured and calculated profiles becomes more and more pronounced. The calculated vertical camera profile becomes broader than the measured profile. A greater degree of asymmetry is observed in the measured profiles.

To investigate the cause of the discrepancy between the measured and modelled profiles it is instructive to analyse in detail the plasma with the highest density (Pulse No:61430), where the discrepancy is most pronounced. Type-I ELMs and n = 1 sawtooth precursors were present in the discharge. Note that the neutron yield depends on the plasma dilution due to the presence of mainly carbon and nickel. TRANSP modelling of the plasma composition using C and Ni as impurities was in agreement with Z_{eff} measurements.

Figures 14 and 15 show the results of TRANSP modelling of the neutron emission for this pulse. As in the previous section it was found that the DT neutron emission before the T beam blip was small (<10%) in comparison with the total neutron flux in this phase. This 'background' DT neutron yield can be reproduced satisfactorily by assuming that the tritium neutrals are only a tiny fraction, ($\sim10^{-4}$) of the all recycling neutrals (see Fig.14a). In contrast with pulses at lower density, a much larger disagreement is found between the modelled and measured neutron fluxes in the DD phase, assuming only neoclassical fast ion diffusion. Assuming anomalous fast ion diffusion in the modelling

reduces this discrepancy, as shown in Fig.14a.

To investigate the effect of anomalous fast ion diffusion on the fast ion distribution function, different assumptions have been made for test purposes only, beginning with the simplest case of an anomalous diffusion coefficient which is constant in time and space, applied to all fast ions. When D_{an} is increased from zero to $5m^2/s$, as can be seen from Fig.14a, the total neutron flux decreases to levels matching the experimental measurements in the deuterium only beam phase. As in all previous cases the neutron flux is significantly overestimated by TRANSP during the tritium beam (DT) phase, and it is necessary to introduce a rather large D_{an}~$10m^2/s$ to match the calculated and measured values from DT reactions, which would be inconsistent with the DD phase. As discussed in previous sections, agreement between measured and calculated neutron flux can be reached by reducing the T beam power by 30-40% depending on the level of the anomalous losses of the fast ions.

To get a better insight in the nature of the anomalous fast ion diffusion, an anomalous diffusion coefficient has been artificially applied to different parts of the fast ion distribution function. Three models have been tried. In the simplest model (**a**) a constant diffusion $D_{an}(r,t)=0$ and $D_{an}(r,t)=5m^2/s$ was applied to all fast ions. The second model (**b**) investigated the effect of losses of trapped particles with energy E>30keV and pitch angle $V_\perp/V > 0.75$ (where $V_\perp$ is the perpendicular velocity and V the total ion velocity) in the equatorial mid-plane on the LFS. The third model (**c**) included the loss, from 15.0 s onwards, of the passing particles with energy E>30keV and $V_{//}/V>0.70$ or $V_\perp/V<0.71$ (where $V_{//}$ is the parallel velocity) in the equatorial mid-plane on the LFS. The effective lifetime of the fast ions was 1ms (τ_f), which is practically equivalent to a prompt loss as $\tau_f << \tau_{sl}$.

Neoclassical behaviour is assumed for the rest of the fast ions in the last two models. Fig.15 and Table 2 show the results of this investigation. Note that the T beam power was varied to reach a minimum χ^2 comparing the measured and simulated neutron profiles. The percentage T power reduction, C_{Tp}, is given for each case in Table 2. A comparison of the measured and modelled neutron emission profiles in Fig.15 shows some discrepancy in the shape for all simulated cases. The trapped ion loss and $D_{an} = 5m^2/s$ (cases (**b**) and (**a**), respectively) produce the largest min(χ^2). The similarity in profile shape improves and min(c^2) decreases in the case (**c**) if losses are assumed for the passing ions only (see Fig.15 and Table 2).). It is clear from Fig.15 that the loss of the trapped ions (case (**b**)) in the simulation creates an excess of the neutrons emitted from the HFS region (channels 11-13) and significant shortage on the LFS (channels 16-19). On the other hand, introducing losses of the passing ions (case (**c**)) skews the modelled profile in the right direction, increasing the number of emitted neutrons on the LFS and reducing it on the HFS. This reproduces some of the features observed in the experimental profile.

As mentioned above MHD activity was observed in the high density ELMy H-mode plasmas discussed in this section. Fig. 16 shows the time evolution of the measured and simulated 14MeV neutron flux, magnetic probe signals for n = 1, 2 modes and D_α signal during the T beam pulse. Analysis of the magnetic and soft X-ray measurements shows that a strong n = 1/m = 1 kink-like mode

at a frequency $f_{n=1} \approx 9$kHz was localised in the plasma core at this time. It exhibits very rapid growth just before the sawtooth crashes at t = 17.018s and t = 17.345s. MHD activity was also observed with higher poloidal mode numbers (m = 2,3; possibly tearing-like mode activity) but the magnetic signals have a significantly lower amplitude,. There is no clear evidence of Alfvénic-type MHD. There is an indication of a saturation in the neutron flux (see Fig.16) during the time interval t = 17.05s to t = 17.15s, which coincides with the increase in n=1 mode activity. However, the same signature can be seen on the modelled neutron flux in the case with zero fast ion anomalous diffusion. Such a correlation in the time evolution of the measured and simulated neutron fluxes does not support a possibility of anomalous diffusion induced by the observed MHD.

The evolution of the fast tritium ion density profile as simulated by TRANSP for a high density H-mode discharge (Pulse No: 61430) is shown in Fig.17a. About 50ms after the start of the T beam, the fast triton density profile reaches a quasi steady state. The profiles are very broad and hollow in contrast to discharges with low or medium plasma density (compare with Fig.8a). The difference can be explained by the shape of the fast triton source profile, which is very broad and hollow in high density H-mode pulses and very peaked in low or medium density optimised shear or hybrid scenario pulses, and one therefore expects greater losses in high density discharges as the fast ions are located closer to the plasma boundary than in discharges with lower density.

The simulated distribution function $F_T(E)$ of the fast tritons is shown in Fig.17b and c as a function of the triton energy for cases (**a**) and (**c**) as described above (see Table). The function in Fig17b is integrated over the radial interval $0.6<r/a<0.9$, full poloidal angle $-\pi \le \theta \le \pi$ and two different pitch angle intervals $(-1<V_{//}/V<0)$ or $(0<V_{//}/V<1)$. Some anisotropy in the pitch angle space $F_T(E, V_{//}/V<0) < F_T(E, V_{//}/V>0)$ is present for cases both with and without anomalous fast triton losses. The asymmetry here is much smaller than in the case of low or medium density plasma (compare Fig.17b and Fig.8b) due to a greater fast ion collisionality. The effect of the anomalous losses of the passing tritons with E>30keV and $V_{//}/V>0.7$ is pronounced in the lower energy part of the $F_T(E)$ and very small in the higher energy part. This can be explained by the fact that the source of the fast beam tritium ions is mainly in a different pitch angle interval. Fast ions are slowed down by a drag force due to interaction with electrons. An effective pitch angle scattering, which populates broader area of $V_{//}/V$, starts only after a significant reduction in energy of the ions. The energy distribution function of fast tritons with $V_{//}/V>0.7$ is shown in Fig.17b. It is, indeed, negligible for E>60keV. Fig.17c demonstrates the poloidal asymmetry in the distribution function of fast tritium ions. The number of the fast tritons on the LFS ($-\pi/2 \le \theta \le \pi/2$) is significantly larger than on the HFS ($\pi/2 \le \theta \le 3\pi/2$) although the integration volume is nearly the same on both sides. This imbalance is directly connected with the large fraction of the trapped fast tritons, which varies from 0.93 to 0.66 during the T beam.

In summary, it should be emphasised that the various assumptions for the losses of passing or trapped ions were introduced to clarify the effect of the losses on the neutron yield and neutron emission profiles. Note that the above method of selectively applying anomalous fast ion losses to different parts of the distribution function is only a first approach. It was shown that assuming

anomalous losses in the the passing fast ion loss skews the profiles in the right direction and improves the similarity in the shape of the measured and modelled profiles. On the contrary, assuming anomalous losses in the trapped particles makes the profile more symmetrical and reduces the similarity with the experiment. More sophisticated models should be tested to verify their adequacy.

CONCLUSIONS

Trace Tritium Experiments on JET allowed a detailed investigation of NB injected fast T ion behaviour by diagnosing 14MeV DT neutron emission, which traces the transport of the T atoms in the plasma. TRANSP simulations for the DD and DT neutron emission rates and DT neutron profiles were compared with measured data for a wide range of plasma parameters in a variety of pulse types including reversed shear, hybrid scenario and standard H-mode and L-mode discharges. TRANSP simulations of the total DD neutron emission rate are consistent with measurements in the phase preceding the T beam for low density discharges $\bar{n}_e < 4\times10^{19}\ m^{-3}$. To reproduce the DT emission during the T beam blip the number of tritons entering the plasma in the simulation had to be artificially reduced by between 20 and 40%, which is large compared to the uncertainty in T beam power. This is, however, not the first time that such an assumption had to be made to fit simulations with the experimental values during T injection and this has been done before in JET and TFTR experiments. No mechanism has yet been proposed that explains such a large reduction. The best match of the measured and calculated DT neutron emission profiles, corresponding to the minimum χ^2, was achieved for the case of small anomalous diffusion $D_{an}<<0.5m^2/s$ in the lower density plasmas. For the H-mode cases with density higher than $\bar{n}_e < 4\times10^{19}\ m^{-3}$ the total neutron emissivity is typically overestimated by TRANSP. It was necessary to introduce a large anomalous diffusivity of the fast ions of the order of $5\text{-}10m^2/s$ to reproduce the total neutron flux in the DD phase of these pulses. To match the total DT neutron flux during the T beam blip, the T beam power was also in this case reduced by 20-40% in the presence of the anomalous losses. Also, the disagreement between the shape of measured and calculated DT neutron profiles becomes more pronounced with increasing density. In particular, profiles measured by the vertical camera are narrower than the corresponding calculated profiles. Introducing anomalous diffusion to all fast ions homogeneously or preferentially to trapped fast ions, increases the minimum χ^2 and reduces the similarity in the profiles shape. However, introducing anomalous losses for the passing fast ions gives the best result in terms of minimisation of χ^2 and profile shape similarity. No evident correlation between the growth of low n/m MHD and reduction of the neutron yield was found. Further analysis of the nature of anomalous fast ion losses is required with the introduction of more sophisticated models in codes.

ACKNOWLEDGEMENT

This work was funded partly by the United Kingdom Engineering and Physical Sciences Research Council and by the European Communities under the contract of Association between EURATOM

and UKAEA. The views and opinions expressed herein do not necessarily reflect those of the European Commission. This work was carried out within the framework of the European Fusion Development Agreement.

REFERENCES

[1]. G.Gorini et al., Proc. 31st EPS Conf. on Plasma Physics, London,UK, ECA, Vol. **28G** (2004)
[2]. E.Ruskov, et al., Phys.Rev.Lett. **82** (1999) 924.
[3]. R.Goldston, et al., J. Comput. Phys. **43** (1981) 61.
[4] S.Guenter, et al., Nucl. Fusion **47** (2007) 920.
[5]. M.Murakami, et al., Phys. Plasmas **13,** (2006) 056106.
[6]. R.Nazikian, et al., 34th EPS Conference, Warsaw, 2007, P1.114
[7]. D.Stork, et al., Nucl. Fusion **45** (2005) 181.
[8]. I.Jenkins, et al., 34th EPS Conference, Warsaw, 2007, P1.150
[9]. N.C.Hawkes, et al., Plasma Phys. Control. Fusion **47** (2005) 1475–1493.
[10]. V.A.Yavorskij, et al., Nucl. Fusion **43** (2003) 1077–1090.
[11]. E.Joffrin, et al. Plasma Phys. Control. Fusion **49** (2007) B629–B649
[12]. M.Adams, et al., Nucl. Instrum .Methods, **A 329** (1993) 277-290.
[13]. O.N. Jarvis, et al., Fusion Eng. Design, **59** (1997), 34-35.
[14]. S.Popovichev, et al., Proc. 31st EPS Conf. on Plasma Physics, London,UK, ECA, Vol. **28G** (2004)
[15]. H Sjostrand et al, Submitted to Nucl. Instrum .Methods, **A**
[16]. M.Greenwald, et al., Nucl. Fusion, **28**, (1988), 2199.
[17]. Tresset G et al., Nucl Fusion **42** (2002) 520
[18]. N.C.Hawkes et al. Plasma Phys. Control. Fusion **44** (2002) 1105
[19]. N.C.Hawkes, et al. Rev. Sci. Instrum. **70 (**1999) 894.
[20]. H.-S.Bosch et al. Nucl.Fusion **32** (1992) 611
[21]. JET Team, Nucl. Fusion, **32**, (1992) 187.
[22]. M.Keilhacker, et al. Nucl. Fusion, **39**, (1999) 209.

Pulse No:	$\bar{n}_e/n_{gr}$	$n_e(0)(10^{19}m^{-3})$	$\bar{n}_e(10^{19}m^{-3})$	I_p (MA)/B_t(T)/q_{95}	$\tau_{sl}(s)^*$
61158	0.4	4.6	3	2.0/2.4/3.7	0.13
61432	0.69	7.5	6.5	2.5/2.7/3.6	0.06
61431	0.86	8.0	8.0	2.5/2.7/3.6	0.05
61427	0.73	8.8	7.7	3.0/2.5/2.8	0.04
61430	0.83	10.2	8.7	3.0/2.5/2.8	0.05

* - $\tau_{sl}(s)$-fast ion slowing down time

Table 1

D_{an} 61430	Case (**a**) 0	Case (**a**) $5m^2/s$	Case (**b**) 1ms life time for trapped fast ions with E>30kEV and $V_{\perp}/V>0.75$ in equatorial mid plain on LFS and (neo)classical behaviour for the rest of the fast ions.	Case (**c**) 1ms life time for passing fast ions with E>30kEV and $V_{//}/V>0.7$ in equatorial mid plain on LFS and (neo)classical behaviour for the rest of the fast ions .
C_{Tp}	35%	27%	13%	14%
$\min(\chi^2)$	2.76	5.31	5.70	2.37

Table 2

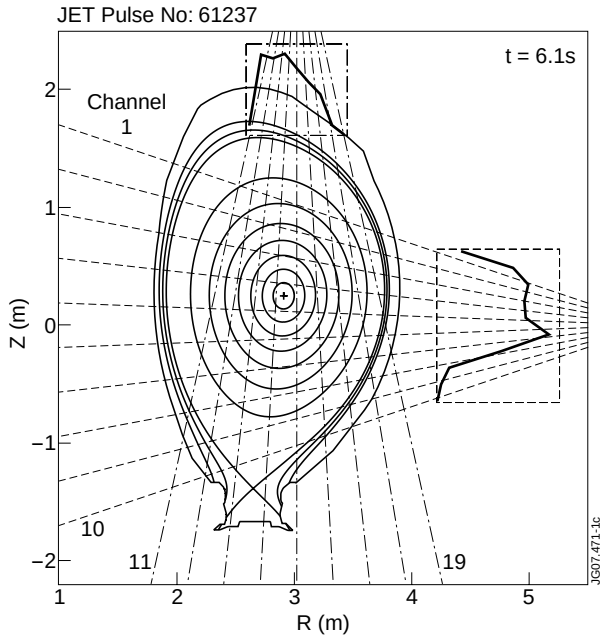

Figure 1: *Lines of sight of the neutron camera on JET with channel numbers and a typical profile shape for off-axis NBI injection.*

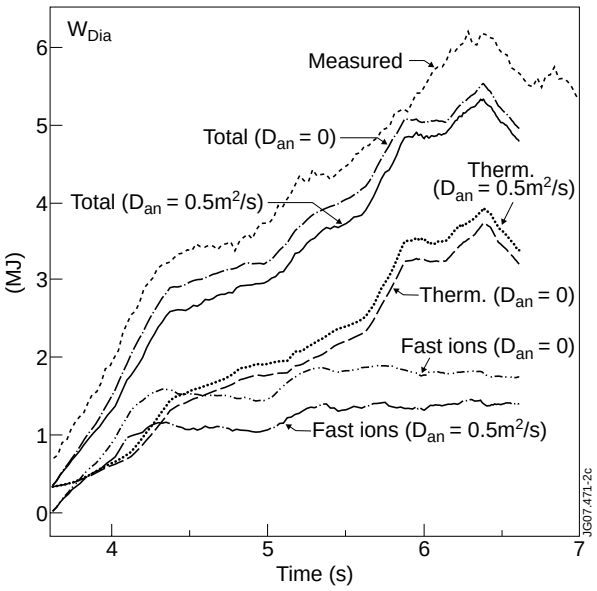

Figure 2: Time traces for the diamagnetic energy W_{dia} , thermal plasma energy and fast ion energy for JET Pulse No: 61341.

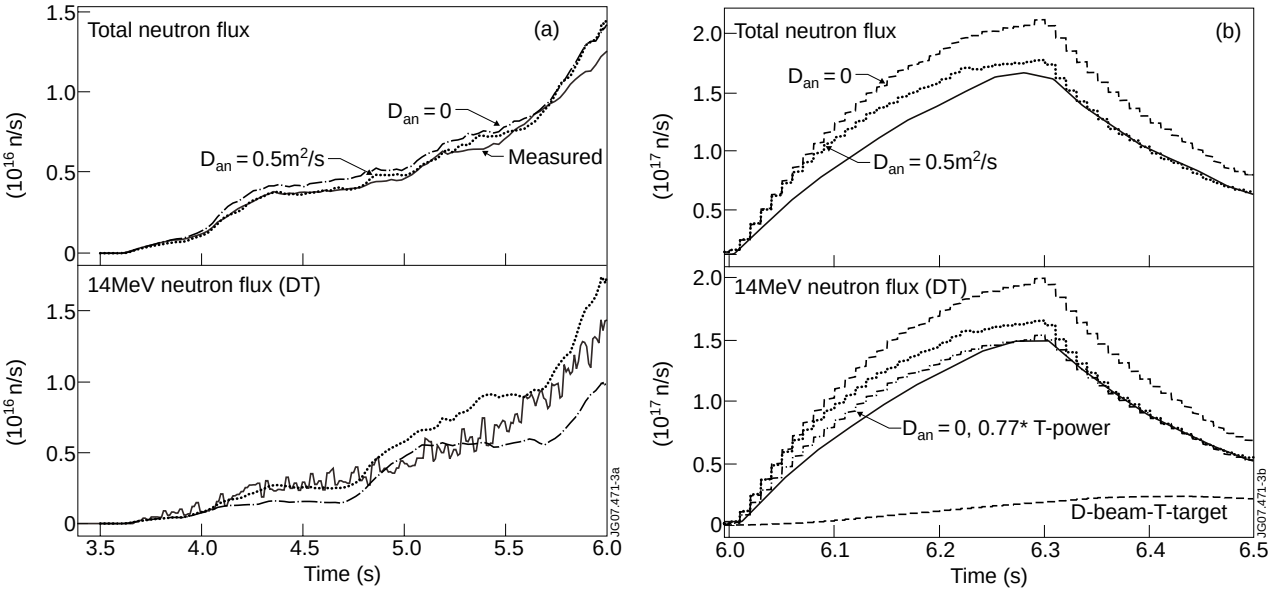

Figure 3: Measured (full lines) and calculated 14MeV neutron rate for Pulse No: 61341, assuming D_{an} = 0 (dashed) or D_{an} = 0.5m/s^2 (dotted) before the T blip (a) and during the T blip (b). For comparison, the calculated 14MeV neutron rate is added for D_{an} = 0 and a 77% reduction of the T beam power (dot-dashed).

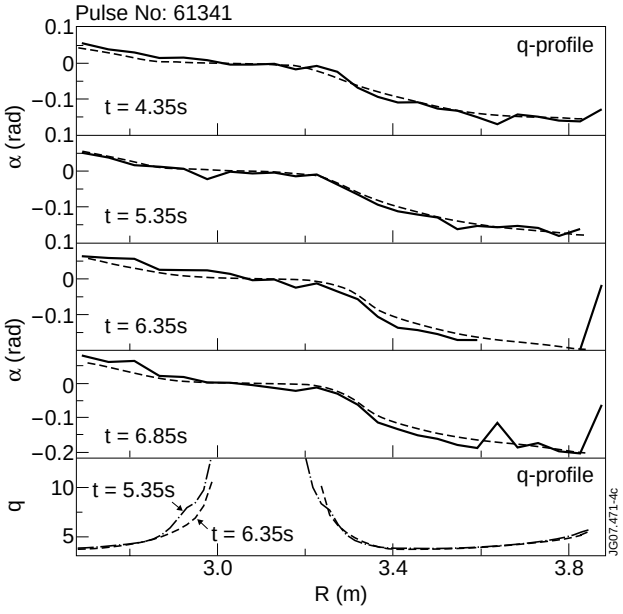

Figure 4: Top 4 boxes show pitch angle a as a function of the major radius at 4 times in the discharge, measured by MSE (full lines) and calculated by TRANSP (dashed lines). Bottom box shows the q-profile for two times close to t=6s in the discharge.

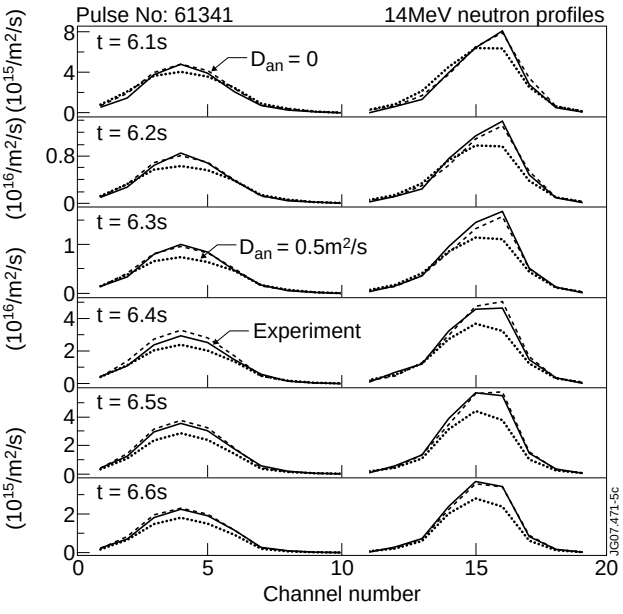

Figure 5: Comparison of calculated and measured 14MeV neutron emission profiles. Pulse No: 61341.

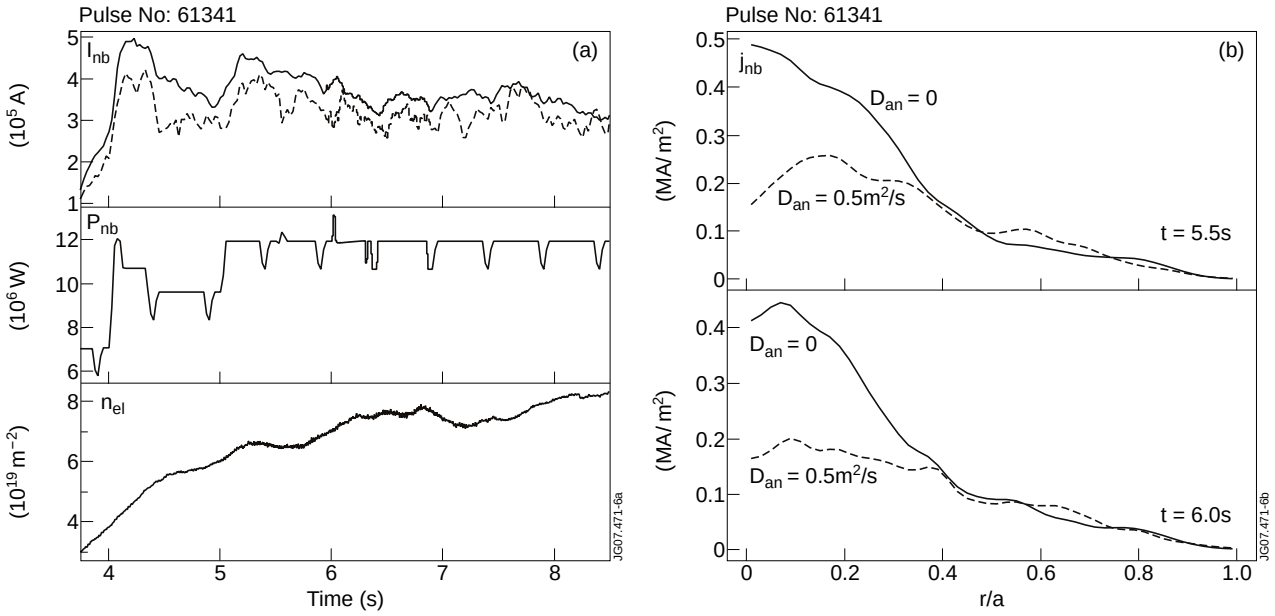

Figure 6: a) TRANSP calculated total beam driven current I_{nb}, injected NB power P_{nb} and line integrated plasma density. b) Beam driven current profiles. Solid line-D_{an}=0, dashed line- D_{an}=0.5m^2/s. Pulse #61341.

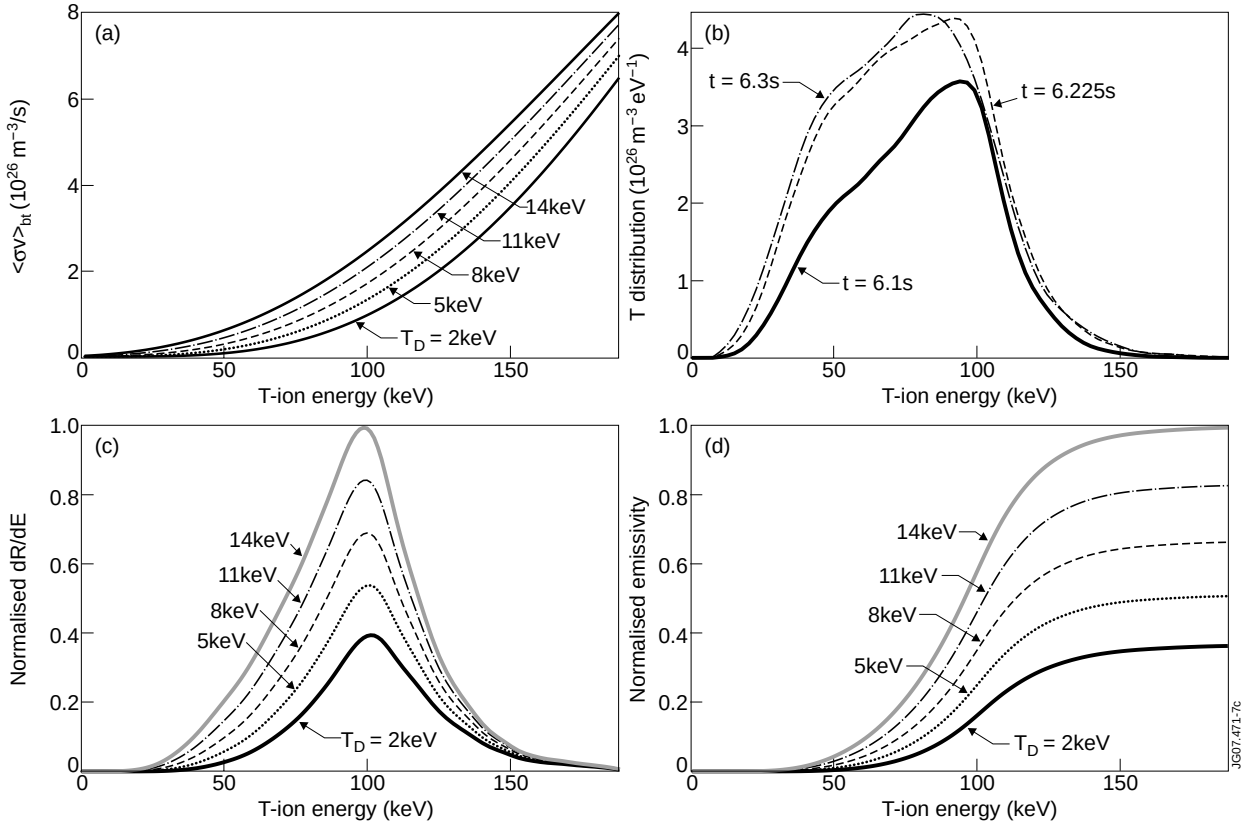

*Figure 7: a) Averaged DT fusion cross section <σ*V> for a T beam in a maxwellian D plasma at temperature T_D as a function of the T beam energy. b) Tritium fast ion distribution function for on-axis injection at 100kV integrated over pitch angle $-1<V_{//}/V<1$, poloidal angle $-\pi<\theta<\pi$ and minor radius $0.1<r/a<0.3$. c) Normalised neutron differential emissivity for the calculated T distribution function in Maxwellian D plasma with a given temperature T_D. Pulse No: 61341, t = 6.225s. d) Normalised neutron emissivity function against beam energy obtained by integrating the function shown in Fig. 1c over the energy. Pulse No: 61341, t = 6.225s*

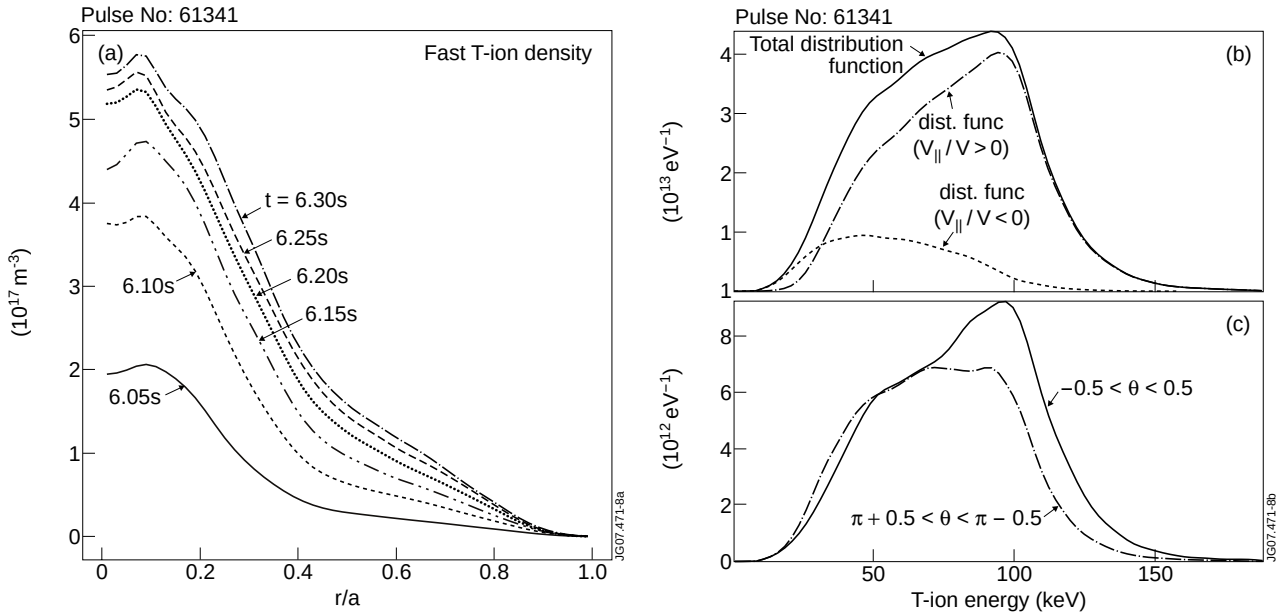

Figure 8: a) Fast tritium ion density variation during T beam blip, b) Tritium fast ion distribution function $F_T(E)$ for on-axis injection at 100kV integrated over poloidal angle $-\pi<\theta<\pi$, minor radius $0.1<r/a<0.3$ and different intervals of pitch angle $V_{//}/V$. c) $F_T(E)$ integrated over poloidal angle $-\pi<\theta<\pi$, minor radius $0.1<r/a<0.3$ and different intervals of pitch angle $V_{//}/V$. Pulse No: 61341, t=6.225s.

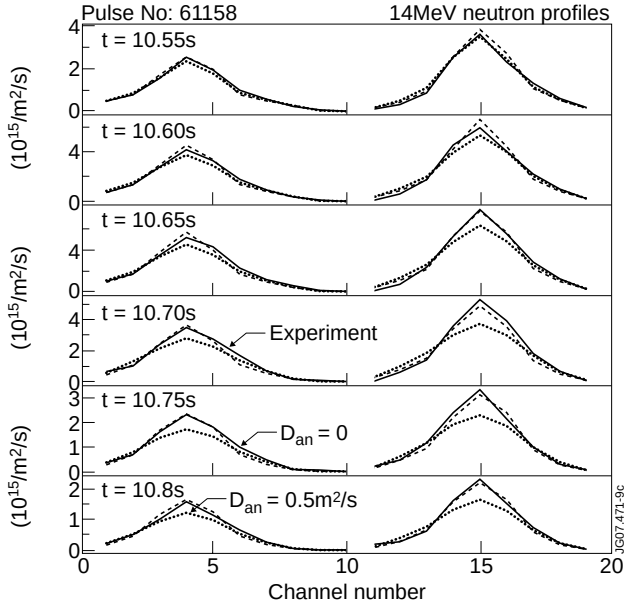

Figure 9: Comparison of calculated and measured 14MeV neutron emission profiles. Pulse No: 61158. Statistical error bars are of the order of 10% or smaller They are shown in Fig. 11b.

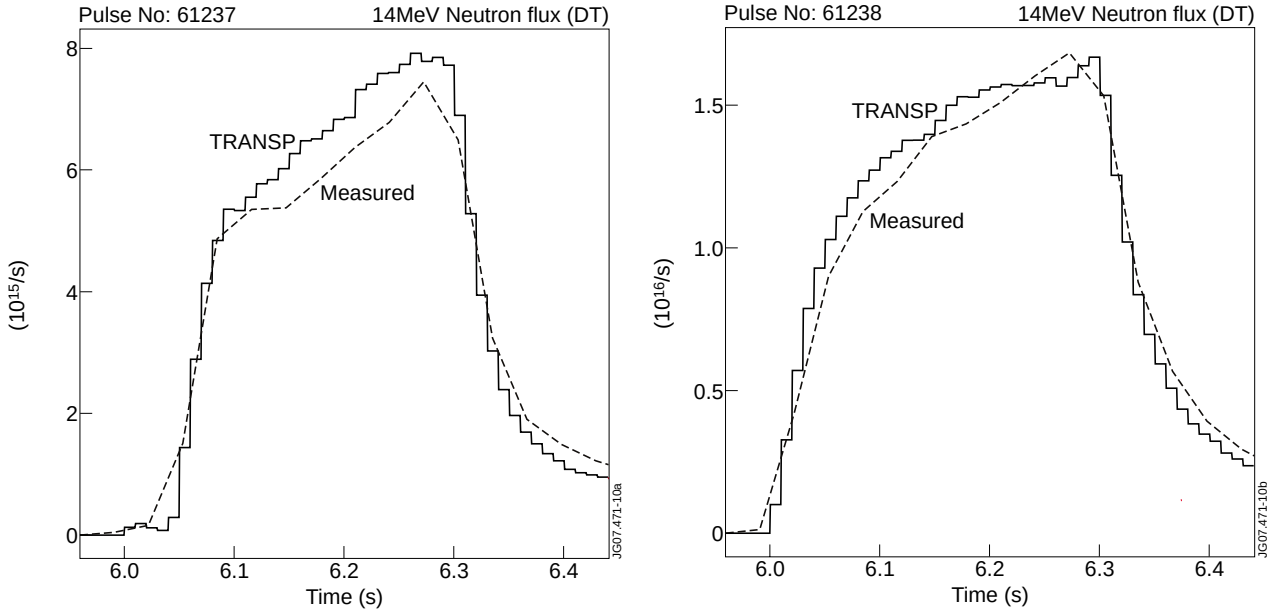

Figure 10: a) Comparison between experimental 14MeV neutron rates and TRANSP simulation for Pulse No's: 61237 (off-axis T, left box) and 61238 (on-axis T, right box).

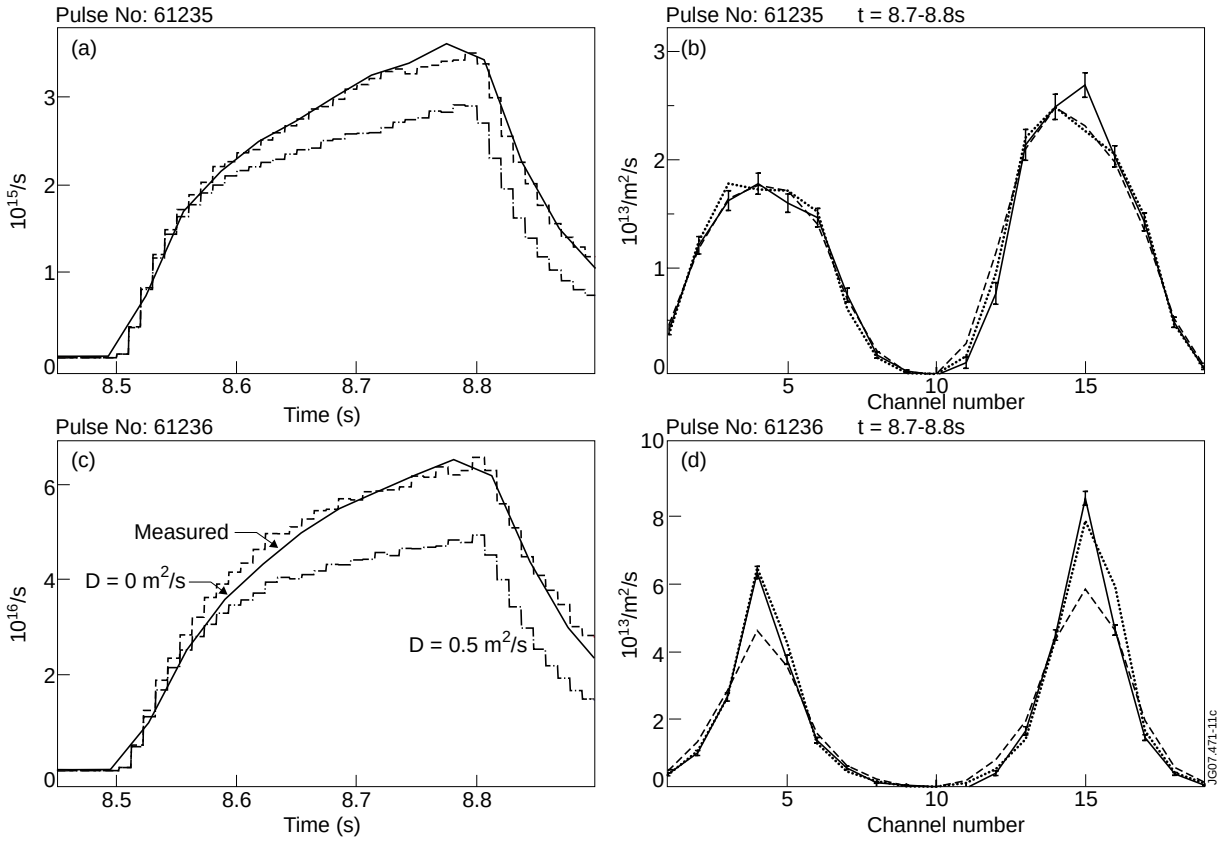

Figure 11: 14MeV neutron rates profiles comparing measured and calculated with $D_{an} = 0$ (dotted) and $D_{an} = 0.5 m^2/s$ (dashed) for Pulse No's: 61235 (off-axis T, Fig11a) and 61236 (on-axis T, Fig.11c) and 14MeV profiles comparing measured (solid) with $D_{an} = 0$ (dotted) and $D_{an} = 0.5 m^2/s$ (dashed) simulation (Fig.11b and 11d). The profiles are integrated over 100ms, the error bars are from a single profile (integrated over 10ms).

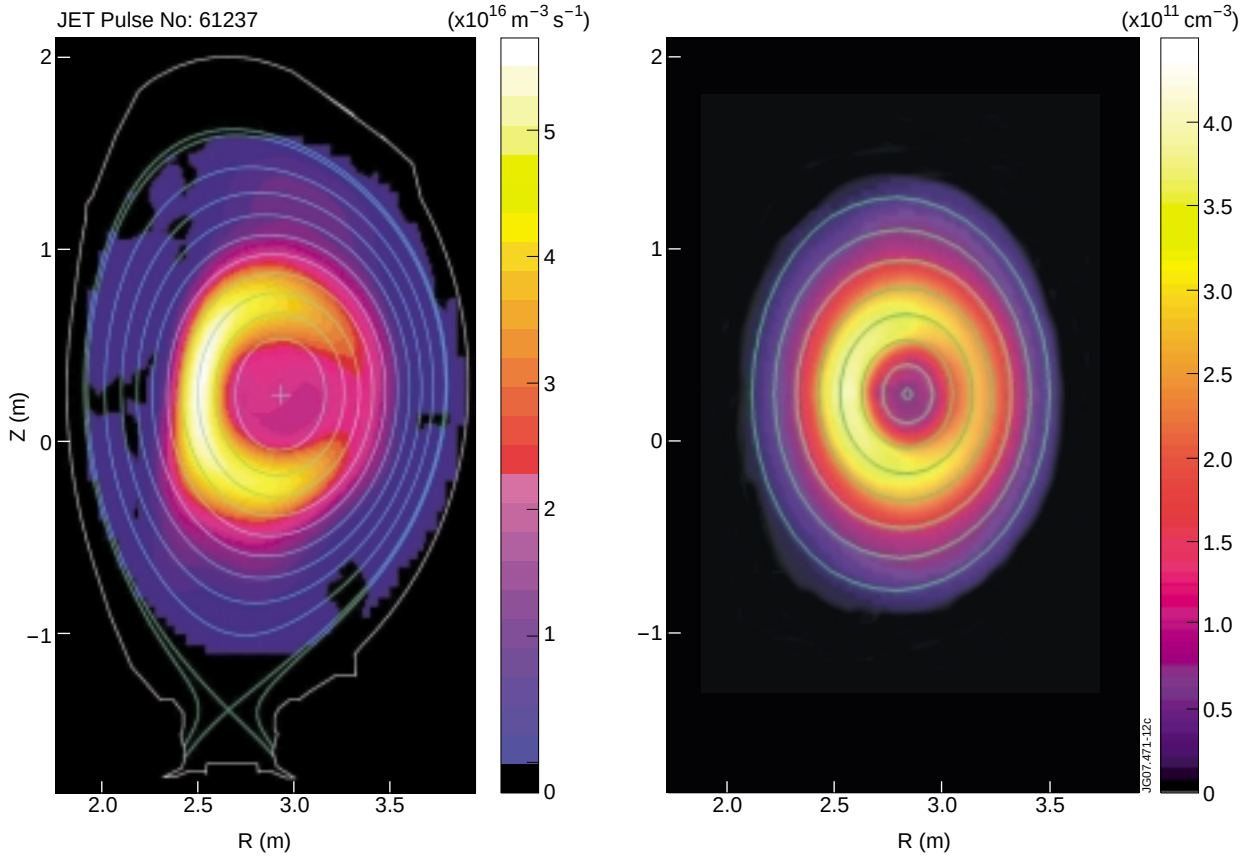

Figure 12: Tomographically inverted experimental 2D neutron emission profile from pulse 61237 at time 6.25s (left) compared with fast ion density in the central plasma region output from TRANSP at the same time and displayed on a simplified up-down symmetric equilibrium (right).

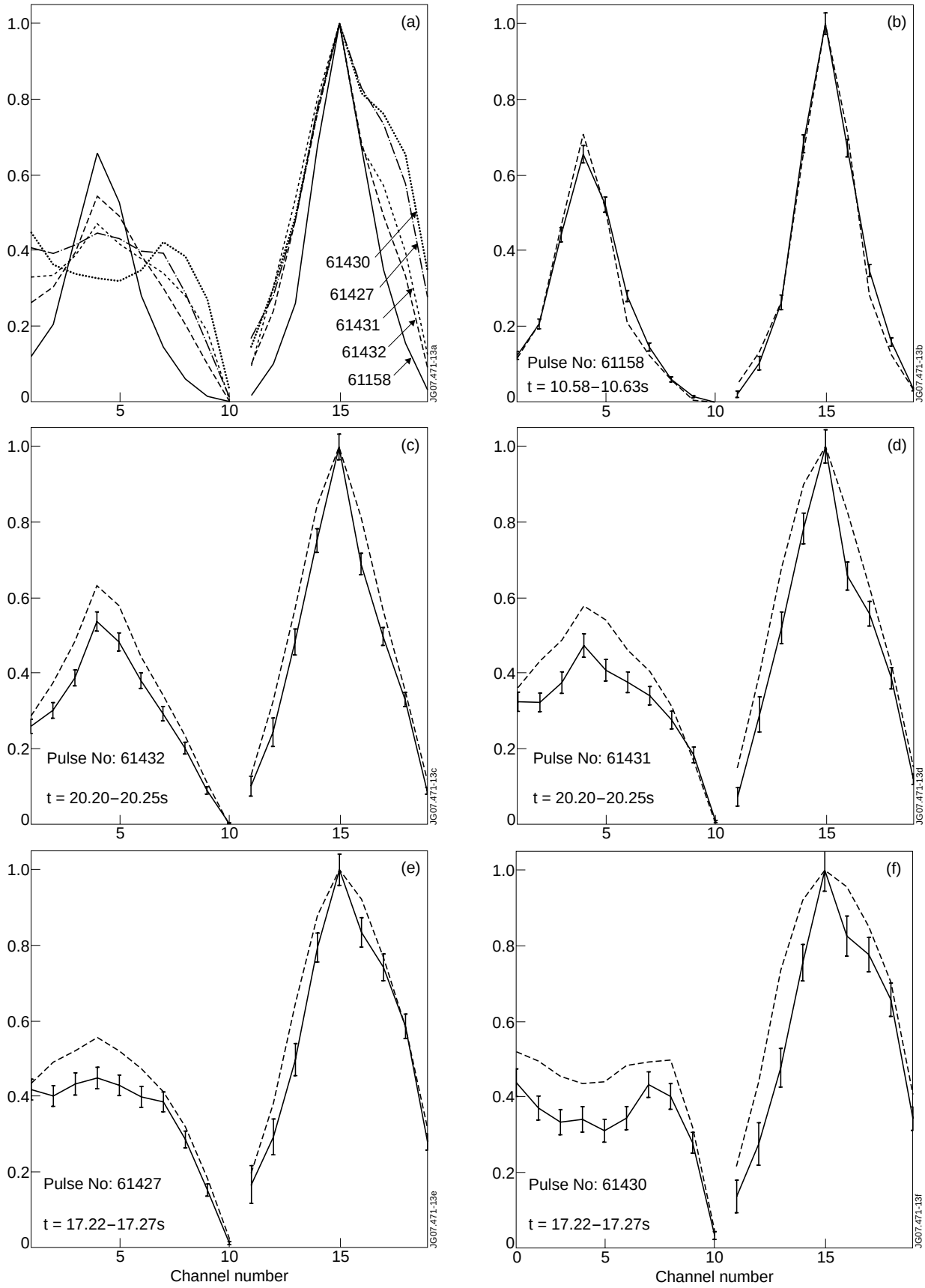

Figure 13: a) Measured 14MeV neutron emission profiles averaged over 50ms, b-f) Comparison of measured (solid line) and calculated (dotted line) profiles with statistical error bars (from 10ms profiles). All profiles are normalised to the maximum value.

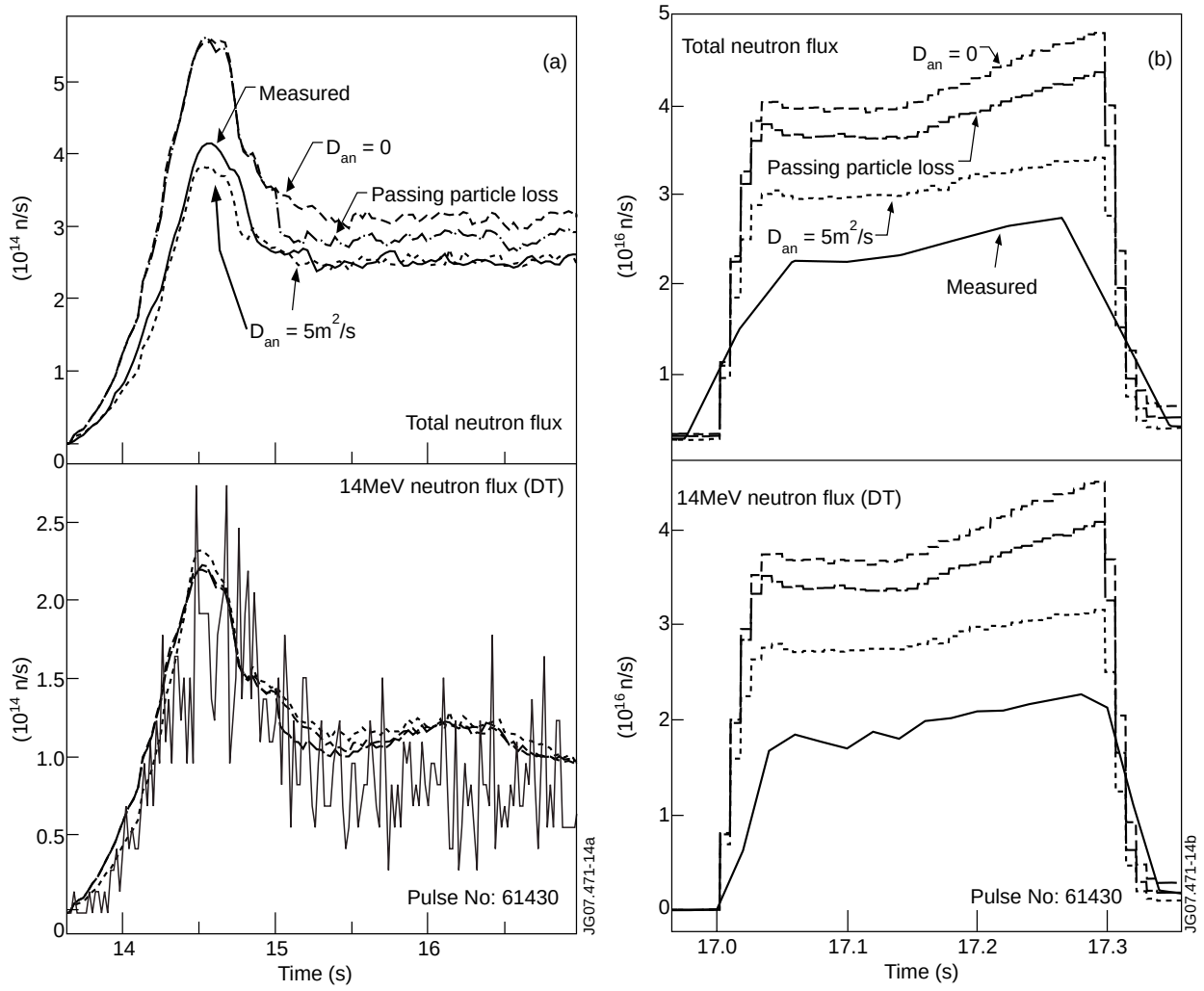

Figure 14: Total neutron rate a)before T blip and b) during and after the blip. Pulse No: 61430. The time resolution of the total neutron flux measurement in b) is coarser than the 14MeV neutron measurement.

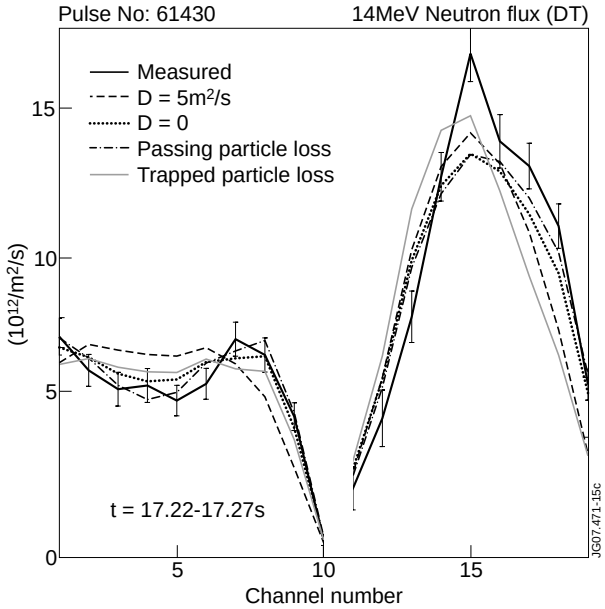

Figure 15: Profiles of 14MeV neutron emission. Pulse No: 61430

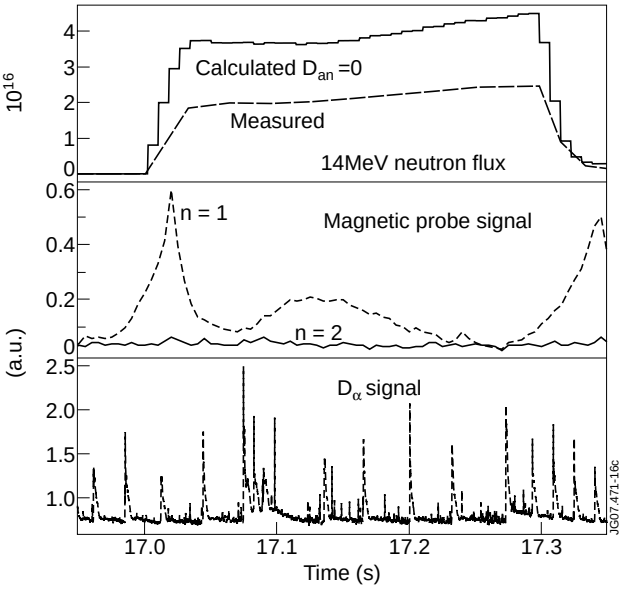

Figure 16: Calculated neutron rate at full T beam power and measured 14MeV neutron flux, magnetic probe signals for n = 1, 2 modes and D_α signal.

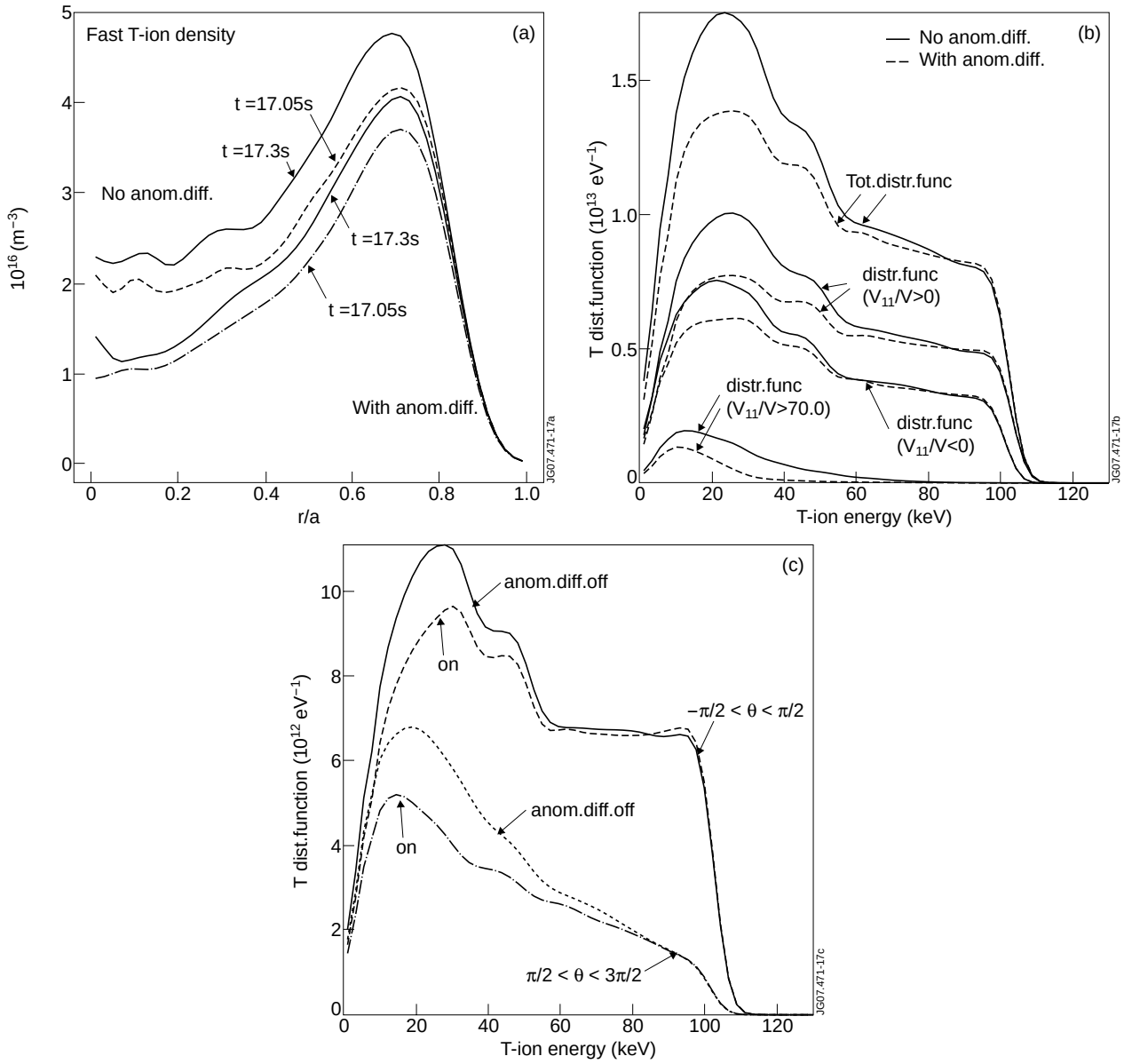

Figure 17: a) Fast tritium ion density variation during T beam blip, b) Tritium fast ion distribution function $F_T(E)$ for on-axis injection at 100kV integrated over poloidal angle $-\pi<\theta<\pi$, minor radius $0.6<r/a<0.9$ and different intervals of pitch angle $V_{//}/V$. c) $F_T(E)$ integrated over minor radius $0.6<r/a<0.9$, pitch angle $-1<V_{//}/V<1$ and different intervals of poloidal angle q. Pulse No: 61430, t = 17.225s.